J. Fluid Mech. (1992), *vol.* 237, *pp.* 301–322
Printed in Great Britain

A $k-\epsilon-\gamma$ equation turbulence model

By JI RYONG CHO AND MYUNG KYOON CHUNG
Department of Mechanical Engineering, Korea Advanced Institute of Science and Technology, Yusong, Taejon, 305-701, Korea

(Received 20 June 1990 and in revised form 17 September 1991)

By considering the entrainment effect on the intermittency in the free boundary of shear layers, a set of turbulence model equations for the turbulent kinetic energy k, the dissipation rate ϵ, and the intermittency factor γ is proposed. This enables us to incorporate explicitly the intermittency effect in the conventional $k-\epsilon$ turbulence model equations. The eddy viscosity ν_t is estimated by a function of k, ϵ and γ. In contrast to the closure schemes of previous intermittency modelling which employ conditional zone averaged moments, the present model equations are based on the conventional Reynolds averaged moments. This method is more economical in the sense that it halves the number of partial differential equations to be solved. The proposed $k-\epsilon-\gamma$ model has been applied to compute a plane jet, a round jet, a plane far wake and a plane mixing layer. The computational results of the model show considerable improvement over previous models for all these shear flows. In particular, the spreading rate, the centreline mean velocity and the profiles of Reynolds stresses and turbulent kinetic energy are calculated with significantly improved accuracy.

1. Introduction

During the last two decades, intensive research effort has been devoted to developing more general computational turbulence models. Unfortunately, however, the predictability of all current turbulence models is still dependent on the flow configuration. For example, even though the flow geometries and boundary conditions of evolving turbulent free shear flows are very simple and well defined, accurate predictions with the available variants of the $k-\epsilon$ or Reynolds stress models invariably require adjustment of the model constants according to the flow geometry, e.g. planar or axisymmetric, as well as to the flow type, e.g. a jet, a wake or a mixing layer.

Specifically, the predictions of a round jet and a plane jet with the same model constants show inconsistent results: if the model constants are adjusted to obtain the correct spreading rate of the plane jet, the computed spreading rate of the round jet is higher than that of the plane jet by as much as 15–25% depending on the computational model. Most experiments indicate, however, that the round jet spreads about 15% slower than the plane jet. This contradictory behaviour of turbulence models in computing the jet flows is termed the *round-jet/plane-jet anomaly* (Pope 1978). A number of attempts to remedy this defect have been made; see Launder *et al.* (1972), McGuirk & Rodi (1977), and Morse (1977). However, since they only modified the model constants in the dissipation equation with reference to the decay rate of the jet centreline mean velocity, general validity of their models to other flows is questionable. Pope (1978) attributed the anomaly in predicting the

round jet to the neglect of the mean vortex stretching effect in the source term of the dissipation equation, and he introduced a vortex stretching invariant term $\chi \equiv (k/\epsilon)^3 \Omega_{ij} \Omega_{jk} S_{ki}$, where Ω_{ij} and S_{ij} are the rate of mean rotation tensor and the rate of mean strain tensor, respectively. The invariant χ is zero in the plane jet, and positive in the round jet. Hence, the turbulent eddy viscosity estimated by $\nu_t \sim k^2/\epsilon$ can be effectively reduced by the increased dissipation rate owing to the positive source term χ in the dissipation equation, and, consequently, the spreading rate can be correctly predicted in a round jet without affecting the predictability for the plane jet. It should be noted that Pope's model constant value of 0.79 was determined by referencing only the round jet in stagnant surroundings. Huang (1986) showed that the adoption of χ deteriorates the computational results for a round jet in a co-flowing stream. Recently, Sohn, Choi & Chung (1991) applied Pope's model in calculating the flow over a ship's hull at the plane of symmetry. The invariant χ becomes positive near the stem and it is negative near the stern, owing to the divergence and convergence of the mean flow, respectively. They found that good prediction can be obtained only when Pope's model constant is re-adjusted to be about 0.4, nearly half the original suggested value. These two investigations reveal that, although Pope's model effectively resolves the round-jet/plane-jet anomaly, the suggested value of the model constant may be too high. Also the model may not be appropriate for round jets with different outer boundary conditions. Noting that the spectral energy transfer rate across the wavenumber, which is nearly equal to the dissipation rate, is significantly promoted by irrotational deformations, Hanjalic & Launder (1980, hereinafter referred to as HL) suggested that in the dissipation equation the effect on the source term for the dissipation by the normal strain is a factor of about 3 greater than that caused by the shear strain. When their model is applied to a round jet, the prediction of the spreading rate is substantially improved, but it is still higher by about 14% than the experimental observation of Rodi (1975). There was another attempt to resolve the anomaly by Hanjalic, Launder & Schiestel (1980, hereinafter referred to as HLS). They suggested dividing the energy-containing part of the spectrum of turbulence into two regions which respond at different rates and in different ways to changes in the mean velocity field. Then two different parts of the $k-\epsilon$ equations were formulated for each region. Their model was termed a two-scale turbulence model. However, the computed spreading rate and the profiles of the computed turbulence quantities did not show any improvement over those of HL. Such anomalous problems with the eddy-viscosity models described above are also common even with the Reynolds stress model; the main source of error has been known to be in the dissipation equation (Launder 1984).

In the 1980–81 AFOSR–HTTM–Stanford Conference on Complex Turbulent Flows (hereinafter, the conference proceeding is referred to as SCP80), another anomaly was found in predicting the simple plane far wake with both the eddy-viscosity model (SCP80, pp. 1306, 1401) and the algebraic Reynolds stress model (SCP80, p. 1401). The plane-wake/plane-jet anomaly is such that, although available experiments show that both flows have similar spreading rates (Rodi 1975), the spreading rate of the plane far wake is under-predicted, by as much as 30% below experimental values, when the model constants are adjusted with respect to the plane jet. The full Reynolds stress model shows the same defect (Launder, Reece & Rodi 1975). Even the models of Pope, HL and HLS which have been proposed to resolve the plane-jet/round-jet anomaly, are not effective in settling the plane-wake/plane-jet anomaly for the following reasons. Pope's model does not work since

the vortex stretching is zero in these plane flows. HL model is not effective for the far wake since the normal strain vanishes in the downstream region. HLS reported that their two-scale model under-predicted the spreading rate of the plane far wake by about 30%. Rodi (1972) recommended an empirically-determined eddy viscosity coefficient which is a local variable and depends on the average ratio of turbulent energy production to dissipation. But the improvement by this model is only marginal (Patel & Scheuerer 1982).

The plane mixing layer was also selected as a target flow for the evaluation of turbulence models in the 1980–81 Stanford Conference. Despite the simplicity of this flow, the computational result posed a fundamental problem for the conventional physical modelling (SCP80, pp. 731, 1400). The computed mean velocity profile by the $k-\epsilon$ model approaches the free-stream velocity too fast near the higher-velocity region, and the predicted Reynolds stresses in this region are much lower than the experimental values. Such a discrepancy was also observed for the Reynolds stress model of Launder *et al.* (1975). The spreading rate was 0.094 with the standard $k-\epsilon$ model, and 0.106 when the model constant $C_{\epsilon 1}$ was changed to match the initial development of the target flow (SCP80, p. 1166). These values are smaller than the experimental value of 0.115, recommended by Birch (SCP80, p. 170).

Another severe problem in calculating the far wake is that the predicted mean defect-velocity drops too rapidly in the outer region. This is common to all turbulence models mentioned above. Patel & Scheuerer (1982) noted that a turbulence model constructed essentially for fully turbulent flows cannot be expected to work in the outer layer contaminated with the irrotational flow. They suggested a new eddy-viscosity relation modified with an intermittency factor, γ. Their model improved the prediction of the mean velocity profile, particularly in the outer region, but the maximum Reynolds shear stress and the spreading rate were still about 25% lower than the experimental values. A theoretical analysis of intermittent flow to derive a computational intermittency model was presented by Libby (1975, 1976) and it was followed by Dopazo (1977) and Chevray & Tutu (1978). A few useful computational schemes were developed at the $k-\epsilon$ level by Byggstoyl & Kollmann (1981), and at the second-order level by Janicka & Kollmann (1983) and Byggstoyl & Kollmann (1986). An alternative approach to take into account the intermittent nature of the flow by utilizing the probability density function has been suggested by Kollmann & Janicka (1982), Pope (1984) and Haworth & Pope (1987). These models reproduce the general behaviour of various free shear flows, and reveal many flow characteristics which cannot be obtained with the conventional turbulence models. However, from the viewpoint of the previous anomalies, all these intermittency models suffer from the same defects as those of the conventional physical modelling.

The present study is aimed at resolving both anomalies described above by including the intermittency factor in the conventional $k-\epsilon$ turbulence model. In order to simplify the discussion of the problem under consideration, our attention is confined to two-dimensional and axisymmetric simple flows. Contrary to the current intermittency modelling method which uses separately the turbulent zone averaged moments and the irrotational zone averaged ones, the conventional Reynolds averaged moments are adopted in our $k-\epsilon-\gamma$ modelling. With this strategy, the number of transport equations to be solved can be reduced, and the present method may be easily extended to other popular higher-order turbulence models.

2. The eddy-viscosity model with the intermittency factor

The eddy viscosity ν_t is basically a phenomenological quantity. From dimensional analysis, it is proportional to a characteristic velocity scale u and a lengthscale l at a point in the flow, i.e. $\nu_t = Cul$, where C is a proportionality constant. At present, the eddy-viscosity model estimated by the turbulent kinetic energy k and the rate of dissipation ϵ is most popular and well established. In this $k-\epsilon$ model, it is assumed that $u \sim k^{0.5}$ and that $l \sim k^{1.5}/\epsilon$. In the intermittent flow region, however, there exists an additional velocity scale of the mean velocity difference between the turbulent fluid and the irrotational one. The effect of such a velocity difference on the eddy viscosity can be conjectured from the following exact shear stress relationships (Chevray & Tutu 1978):

$$\overline{u_i u_j} = \gamma\overline{\widetilde{u_i u_j}} + (1-\gamma)\overline{\widetilde{u_i u_j}} + \gamma(1-\gamma)(\overline{\widetilde{U}}_i - \overline{\widetilde{U}}_i)(\overline{\widetilde{U}}_j - \overline{\widetilde{U}}_j) \quad (i \neq j), \tag{2.1}$$

where $\approx$ and $\simeq$ denote the turbulent and the irrotational (or non-turbulent) zone averages, respectively. The sum of the first and second terms on the right-hand side represents the momentum transport due to the fluctuating velocity. Hence, the usual gradient transport approximation may be applied as follows:

$$\gamma\overline{\widetilde{u_i u_j}} + (1-\gamma)\overline{\widetilde{u_i u_j}} \simeq 2F_1(\gamma)\, ulS_{ij} \quad (i \neq j), \tag{2.2}$$

where $S_{ij} = \frac{1}{2}(U_{i,j} + U_{j,i})$. In obtaining this relation, we have further assumed that the turbulent and the irrotational zone momentum transports together can be approximated by the conventional Reynolds averaged quantities with an unknown functional coefficient $F_1(\gamma)$. The last term of (2.1) reveals that the mean velocity difference between the two fluids contributes also to the momentum transport by the bulk convective motion. Lumley (1980) supposed that the velocity 'jump' is caused by the intermittency gradient and by the mean velocity 'jump' itself:

$$\overline{\widetilde{U}}_i - \overline{\widetilde{U}}_i = -F_2(\gamma)\frac{k^2}{\epsilon}\frac{\partial\gamma}{\partial x_i} - F_3(\gamma)\frac{k}{\epsilon}(\overline{\widetilde{U}}_j - \overline{\widetilde{U}}_j)\frac{\partial U_i}{\partial x_j}, \tag{2.3}$$

where $F_2(\gamma)$ and $F_3(\gamma)$ are unknown functions. From the above three equations, the following relation can be obtained for a thin shear flow:

$$-\overline{u_i u_j} = 2F_1 ul\left[1 + \gamma(1-\gamma)\frac{F_2^2 F_3}{2F_1} l^2 \frac{\partial\gamma}{\partial x_k}\frac{\partial\gamma}{\partial x_k}\right] S_{ij} \quad (i \neq j), \tag{2.4}$$

where the intermittency gradient originates from the mean velocity jump, and the bracketed term may be understood as a correction to the velocity scale. From this basic functional form, we propose the following eddy viscosity relation:

$$-\overline{u_i u_j} = 2\nu_t S_{ij} \quad (i \neq j), \tag{2.5}$$

where

$$\nu_t = C_\mu\left[1 + C_{\mu g}\frac{k^3}{\epsilon^2}\gamma^{-m}(1-\gamma)\frac{\partial\gamma}{\partial x_k}\frac{\partial\gamma}{\partial x_k}\right]\frac{k^2}{\epsilon} = C'_\mu\frac{k^2}{\epsilon}. \tag{2.6}$$

The data of Rodi (1975, p. 147) show that the parameter C'_μ increases monotonously to infinity in the outer region of free shear layers where the intermittency factor decreases from one to zero. Since the cross-stream gradient of γ is approximately proportional to $\gamma(1-\gamma)$ for the free-boundary-layer-type flows (Byggstoyl &

Kollmann 1981), and since the lengthscale $l(\sim k^{1.5}/\epsilon)$ is fairly constant in this region, it is necessary to have $m > 2$ in order to reproduce the observed variation of C'_μ in Rodi (1975). By referencing the eddy-viscosity distribution in the intermittent region of a plane jet (Ramaprian & Chandrasekhara 1985), the value of m was selected to be 3, approximately. Note that the above eddy-viscosity model reduces to the usual form in the fully turbulent zone where $\gamma = 1.0$.

3. The intermittency equation

Although Libby (1975) postulated a transport equation for the intermittency factor, the exact formulation has been provided by Dopazo (1977) by conditioning the instantaneous continuity equation with an intermittency indicator function. The indicator function is a train of pulses denoting 'one' and 'zero' as the passage of turbulent and irrotational fluid, respectively, at a given point in the flow field. According to him, the intermittency equation is a continuity equation for the turbulent fluid alone, and it reads:

$$U_j \frac{\partial \gamma}{\partial x_j} = D_g + S_g, \tag{3.1}$$

where

$$D_g \equiv \frac{\partial}{\partial x_j}[-\gamma(1-\gamma)(\widetilde{\overline{U}}_j - \widetilde{\overline{U}}_j)], \tag{3.2}$$

and

$$S_g \equiv \lim_{\text{vol}\to 0} \frac{1}{\text{vol}} \overline{\int_s V_e \, dS}. \tag{3.3}$$

In (3.3), V_e is the speed of advance of the turbulent–irrotational interface $S(\boldsymbol{x}, t)$ relative to the fluid element. D_g represents the spatial transport of the intermittency factor γ owing to the mean velocity jump between the two fluids. If the convection velocity in (3.1) is taken as the turbulent zone mean velocity, the term D_g vanishes. With the aid of Lumley's velocity jump model of (2.3), Byggstoyl & Kollmann (1981) proposed estimating D_g for thin shear flows by the following diffusion model:

$$D_g = \frac{\partial}{\partial x_j}\left[(1-\gamma)\frac{\nu_t}{\sigma_g}\frac{\partial \gamma}{\partial x_j}\right], \tag{3.4}$$

The second term S_g in (3.1) represents the conversion rate of the irrotational fluid to the turbulent one per unit volume. A model for the source term, S_g, was first proposed by Libby (1975) and then investigated by Chevray & Tutu (1978), Lumley (1980), Byggstoyl & Kollmann (1981, 1986) and Pope (1984). Among them, the model of Byggstoyl & Kollmann (1986) has been widely applied to various flows. In the present study, their model is slightly modified to have the following form:

$$S'_g = C_{g1}\gamma(1-\gamma)\frac{P_{k,s}+P_{k,n}}{k} + C_{g2}\frac{k^2}{\epsilon}\frac{\partial \gamma}{\partial x_j}\frac{\partial \gamma}{\partial x_j}, \tag{3.5}$$

where $P_{k,s}$ and $P_{k,n}$ represent the production of turbulent kinetic energy by the shear and normal strains, respectively, and they are defined in (4.2). The first term in the right-hand side of (3.5) expresses the generation of γ owing to the production of the turbulent kinetic energy. The second term represents the increase of γ by the spatial inhomogeneity or the gradient of γ itself. Equation (3.5) differs from the original

version of Byggstoyl & Kollmann (1986) in that the turbulent zone quantities are simply replaced by the respective unconditional averages. Another difference is that the sink term, $-C'\gamma(1-\gamma)\epsilon/k$, in their original model has been dropped. The reason is that such a destruction effect can be included implicitly in the first source term by decreasing the model constant C_{g1} since $\epsilon \simeq (P_{k,s}+P_{k,n})$ is a fairly good approximation in the outer region of free shear flows.

Evidently, the intermittency at a point must be dependent on entrainment of the surrounding irrotational fluid as well as on the spatial transport D_g and the source like S'_g in (3.5). However, (3.1), together with models (3.4) and (3.5), does not include the important contribution from such an entrainment process. The transport of intermittency by the entrained mass is similar to that by the convective motion. At the first stage of the mass entrainment process, the smallest-scale eddies cause the contortion of the turbulent–irrotational interface, therefore, viscosity acts to propagate vorticity into the irrotational fluid. At the later stage, however, the net rate of propagation or entrainment is controlled by the speed at which the contortions with largest scales move into the surrounding fluid. The organized eddies with their axes parallel to the direction of extension by the mean velocity gradient are more effective for the entrainment than the randomly oriented eddies. Eventually, the presence of the mean velocity gradient dominates the intermittency transport by the entrainment (Townsend 1976, p. 235). Meanwhile, since the mass entrainment is a passive process, the overall entrainment velocity must be proportional to the negative of the maximum mean pressure slope, $-\nabla(P/\rho)$, where P is the mean static pressure and ρ is the fluid density. Here, the gradient of P may be determined by the Bernoulli relation for nearly irrotational incompressible flow:

$$-\nabla(P/\rho) \approx \nabla(\tfrac{1}{2}\boldsymbol{U}\cdot\boldsymbol{U}). \tag{3.6}$$

It has been shown by Tennekes & Lumley (1972, p. 119) and Townsend (1976, p. 247) that the entrainment velocity is also proportional to the relative turbulent intensity, $k^{0.5}/|\boldsymbol{U}|$. In addition, the transported intermittency at a given point by the entrained mass should be proportional to $-\nabla\gamma$. Consequently, the interaction between the mean velocity gradient and the intermittency field contributes to transport the intermittency by an amount,

$$S_\gamma = C_{g3}\frac{k^{\frac{1}{2}}}{|\boldsymbol{U}|}\nabla(\tfrac{1}{2}\boldsymbol{U}\cdot\boldsymbol{U})\cdot(-\nabla\gamma)\frac{k}{\epsilon}\gamma(1-\gamma)$$

$$= C_{g3}\gamma(1-\gamma)\frac{\epsilon}{k}\Gamma, \tag{3.7}$$

where

$$\Gamma \equiv \frac{k^{\frac{5}{2}}}{\epsilon^2}(\nabla|\boldsymbol{U}|)\cdot(\nabla\gamma) = \frac{k^{\frac{5}{2}}}{\epsilon^2}\frac{U_i}{(U_k\,U_k)^{\frac{1}{2}}}\frac{\partial U_i}{\partial x_j}\frac{\partial\gamma}{\partial x_j}. \tag{3.8}$$

In (3.7), $\gamma(1-\gamma)k/\epsilon$ has been multiplied for dimensional requirement and for physical consistency with the fully turbulent fluid or fully irrotational one. The newly defined quantity Γ may be interpreted as a non-dimensional invariant of the interaction which represents the amount of intermittency entrained by the interaction between the mean velocity gradient and the intermittency field per unit volume of fluid. It is noted that when the frame of reference is moving at a constant velocity $\boldsymbol{U}_F$, then the velocity $\boldsymbol{U}$ in (3.8) must be replaced by $\boldsymbol{U}-\boldsymbol{U}_F$ to secure the Galilian invariance of the scalar Γ. Note that the final form of S_γ in (3.7) is consistent

with the physical reasoning described above. Now, then, the source S_g in (3.1) can be represented by the following equation:

$$S_g = S'_g + S_\gamma$$
$$= C_{g1}\gamma(1-\gamma)\frac{P_{k,s}+P_{k,n}}{k} + C_{g2}\frac{k^2}{\epsilon}\frac{\partial\gamma}{\partial x_j}\frac{\partial\gamma}{\partial x_j} - C_{g3}\gamma(1-\gamma)\frac{\epsilon}{k}\Gamma. \tag{3.9}$$

4. The dissipation equation for the turbulent kinetic energy

Since we are interested in working out the anomalies in computing turbulent free shear flows, we start with the following dissipation equation which includes both HL's preferential normal strain term and Pope's (1978) vortex stretching invariant.

$$U_j\frac{\partial\epsilon}{\partial x_j} = \frac{\partial}{\partial x_j}\left[\frac{\nu_t}{\sigma_\epsilon}\frac{\partial\epsilon}{\partial x_j}\right] + \frac{\epsilon^2}{k}\left[C_{\epsilon1}\frac{P_{k,s}+3P_{k,n}}{\epsilon} - C_{\epsilon2} + C_{\epsilon3}\chi\right], \tag{4.1}$$

where
$$P_{k,s} = -\overline{u_i u_j}\frac{\partial U_i}{\partial x_j} \quad (i \neq j), \quad P_{k,n} = -\overline{u_i u_j}\frac{\partial U_i}{\partial x_j} \quad (i = j), \tag{4.2}$$

$$\chi = (k/\epsilon)^3\Omega_{ij}\Omega_{jk}S_{ki}, \tag{4.3}$$

$$\Omega_{ij} = \frac{1}{2}\left[\frac{\partial U_i}{\partial x_j} - \frac{\partial U_i}{\partial x_i}\right], \quad S_{ij} = \frac{1}{2}\left[\frac{\partial U_i}{\partial x_j} + \frac{\partial U_i}{\partial x_i}\right]. \tag{4.4}$$

When this equation was utilized in calculating turbulent free shear flows with the $k-\epsilon$ model or the Reynolds stress model during the initial stage of the present work, it turned out that the calculated dissipation rate was lower than the experimental value in the jet, and higher in the wake. Such a discrepancy is thought to be the critical source of the anomalies, which suggests that there should be another physical mechanism participating in the dissipative process.

Extending the discussion about the intermittency as given in §3, undoubtedly, the rate of dissipation at a point must also depend on the level of intermittency. When the intermittency is low, the small-scale eddies are relatively inactive and the turbulent kinetic energy is slowly dissipated. However, when it is high, the energy dissipation should be increased by the presence of the fine scale eddy motions embedded in the energetic large straining eddies in the interactive shear layer between the turbulent and irrotational zones. One of the most convenient measures of such an additive source (or sink) of dissipation owing to the entrainment of more-irrotational fluid into that point under consideration is the intermittency interaction invariant Γ. Therefore, it is suggested that one more source (or sink) term be added in the right-hand side of (4.1) as follows:

$$U_j\frac{\partial\epsilon}{\partial x_j} = \frac{\partial}{\partial x_j}\left[\frac{\nu_t}{\sigma_\epsilon}\frac{\partial\epsilon}{\partial x_j}\right] + \frac{\epsilon^2}{k}\left[C_{\epsilon1}\frac{P_{k,s}+3P_{k,n}}{\epsilon} - C_{\epsilon2} + C_{\epsilon3}\chi + C_{\epsilon4}\Gamma\right]. \tag{4.5}$$

It is worthwhile discussing the intermittency invariant term in the above model equation from the viewpoint of the lengthscale variation. Consider the two different cases depicted in figures 1(*a*) and (*b*). In the case of a jet in figure 1(*a*), the inner product between the entrainment vector, $-\nabla(P/\rho)$, and the intermittency gradient vector, $\nabla\gamma$, is positive and the pressure field drives more-irrotational fluid towards the more-turbulent region. Hence, the cross-stream position at which $\gamma = 0.5$ is shifted inward. Since the lengthscale of turbulence l is proportional to the cross-

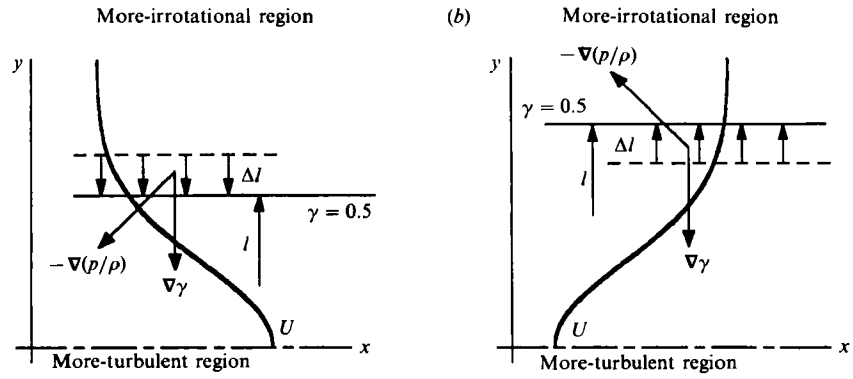

FIGURE 1. An interaction effect of mean shear and intermittency fields.

stream distance of the point where $\gamma = 0.5$ from the jet centreline, the inward movement of the more-irrotational fluid effectively decreases the lengthscale. In (4.5), the positive value of the intermittency invariant term for case 1(*a*) acts as a source of ϵ, thus ϵ is increased. Therefore, from the relation, $l \sim k^{\frac{3}{2}}/\epsilon$, it turns out that the lengthscale does decrease. Similarly, figure 1(*b*) shows the converse case which represents the wake flow. Here, the inner product $-\nabla(P/\rho)\cdot\nabla\gamma$ becomes negative and the dissipation is reduced; thus, the lengthscale increases owing to the outward movement of the more-turbulent fluid.

5. Applications of the proposed model to turbulent free shear flows

The present $k-\epsilon-\gamma$ equation model is applied to compute various two-dimensional and axisymmetric turbulent free shear flows, namely, a plane jet, a round jet, a plane far wake and a plane mixing layer. For these thin-boundary-layer-type flows at high Reynolds number, the streamwise momentum equation and the turbulent kinetic energy equation are as follows:

$$U\frac{\partial U}{\partial x}+V\frac{\partial U}{\partial y}=\frac{1}{r}\frac{\partial}{\partial y}\left[r\nu_t\frac{\partial U}{\partial y}\right]-\frac{\partial}{\partial x}(\overline{u^2}-\overline{v^2}), \tag{5.1}$$

$$U\frac{\partial k}{\partial x}+V\frac{\partial k}{\partial y}=\frac{1}{r}\frac{\partial}{\partial y}\left[r\frac{\nu_t}{\sigma_k}\frac{\partial k}{\partial y}\right]+P_{k,s}+P_{k,n}-\epsilon, \tag{5.2}$$

where r is the radial distance from the centreline for axisymmetric flows, and it is 1 for plane flows. The productions of turbulent kinetic energy are given by

$$P_{k,s}=-\overline{uv}\frac{\partial U}{\partial y},\quad P_{k,n}=-(\overline{u^2}-\overline{v^2})\frac{\partial U}{\partial x}. \tag{5.3}$$

Following HL, the normal stress difference may be approximated as a constant fraction of the turbulent kinetic energy, or

$$(\overline{u^2}-\overline{v^2})=C_{uv}k. \tag{5.4}$$

After transforming the governing equations to a similarity coordinate η, the numerical solutions are obtained by integrating numerically the resulting nonlinear ordinary differential equations with the tri-diagonal matrix algorithm. For each flow configuration, a stream function $\Psi(x,\eta)$ is defined in the same way as Rajaratnam (1976). Then, the dependent variables $U(x,y)$, $k(x,y)$, $\epsilon(x,y)$, $\gamma(x,y)$ and $\nu_t(x,y)$ are

transformed to the similarity variables $W(\eta)$, $K(\eta)$, $E(\eta)$, $G(\eta)$ and $D(\eta)$ in table 1, respectively. A preliminary computation in the η-coordinate showed wavelike unstable solutions near the outer edge because of the vanishing of the turbulent kinetic energy and its dissipation rate. This edge singularity in obtaining the similarity solution was also observed by Paullay *et al.* (1985) for the usual $k-\epsilon$ model and by Stuttgen & Peters (1987) for Rotta's $k-l$ model. Paullay *et al.* (1985) introduced a transformation that stretches the finite edge to infinity and decouples the system of equations, thereby the numerical integration becomes stable and efficient. The transformation is $\eta = \eta(\zeta)$, where

$$\frac{\mathrm{d}\eta}{\mathrm{d}\zeta} = \nu_t, \quad \eta = \int_0^\zeta \nu_t \,\mathrm{d}\zeta. \tag{5.5}$$

When the governing equations are transformed to the ζ-coordinate, the resulting equations can be generally represented as

$$-A\phi - B\frac{\mathrm{d}\phi}{\mathrm{d}\zeta} = \frac{\mathrm{d}}{\mathrm{d}\zeta}\left[C\frac{\mathrm{d}\phi}{\mathrm{d}\zeta}\right] + S. \tag{5.6}$$

Since the procedure of the coordinate transformation from (x, y)-coordinates to (x, ζ)-coordinates is direct but lengthy, it is not described here. The coefficients A, B, C and S are summarized in table 2. The similarity variable for the eddy viscosity relation of (2.6) is given by

$$D(\zeta) = C_\mu\left\{1 + C_{\mu g}\frac{K^3}{E^2}\frac{1-G}{G^3}\left(\frac{1}{D}\frac{\mathrm{d}G}{\mathrm{d}\zeta}\right)^2\right\}\frac{K^2}{E}. \tag{5.7}$$

Similarity variables for source terms in the k, ϵ and γ equations are represented by the following equations,

$$S_k(\zeta) = P_{k,s}(\zeta) + P_{k,n}(\zeta) - E(\zeta), \tag{5.8}$$

$$S_\epsilon(\zeta) = \frac{E^2}{K}\left[C_{\epsilon 1}\frac{P_{k,s} + 3P_{k,n}}{E} - C_{\epsilon 2} + C_{\epsilon 3}\chi(\zeta) + C_{\epsilon 4}\Gamma(\zeta)\right], \tag{5.9}$$

$$S_g(\zeta) = C_{g1}G(1-G)\frac{P_{k,s} + P_{k,n}}{K} + C_{g2}\frac{K^2}{E}\left(\frac{1}{D}\frac{\mathrm{d}G}{\mathrm{d}\zeta}\right)^2 - C_{g3}G(1-G)\frac{E}{K}\Gamma(\zeta). \tag{5.10}$$

The functional forms of $P_{k,s}(\zeta)$, $P_{k,n}(\zeta)$, $\chi(\zeta)$ and $\Gamma(\zeta)$ are summarized in table 3, and the boundary conditions are listed in table 4. At the symmetry boundary ($\zeta = 0$), reflecting boundary conditions are invoked for all dependent variables except the mean velocity for which $W(\zeta = 0) = 1$. At the free boundary edge, the asymptotic value for the dependent variable is related to the inner grid value by analysing the behaviour of the transformed governing equation near the edge region (Paullay *et al.* 1985).

In order to test the grid dependence of the computations, all target flows were computed with four different numbers of grid points; namely, 80, 100, 150 and 200 cross-stream nodes. All these test runs showed 0.5% variations in the maximum Reynolds shear stresses, and the computed results with 150 nodes are reported in the present paper. The convergence of solutions was checked by the criterion, $\Sigma|\phi_{new} - \phi_{old}|/\Sigma|\phi_{new} + \phi_{old}| < 10^{-6}$, for all dependent variables ϕ.

In the above model equations, most of the empirical model constants are assigned by previously established values as summarized in table 5. The present intermittency model requires three additional model constants, $C_{\mu g}$, C_{g3} and $C_{\epsilon 4}$. The constant $C_{\mu g}$

	Plane jet	Round jet	Plane wake	Mixing layer
η	y/x	y/x	$y/(\theta x)^{\frac{1}{2}}$	y/x
$\Psi(x,\eta)$	$U_0(x)xF(\eta)$	$U_0(x)x^2F(\eta)$	—	$U_M xF(\eta)$
$U(x,y)$	$U_0(x)W(\eta)$	$U_0(x)W(\eta)$	$U_\infty - U_d(x)W(\eta)$	$U_M W(\eta)$
$W(\eta)$	$\dfrac{dF}{d\eta}$	$\dfrac{1}{\eta}\dfrac{dF}{d\eta}$	$U_d(x) \equiv U_\infty Q(\theta/x)^{\frac{1}{2}}$	$\dfrac{dF}{d\eta}$
$V(x,y)$	$U_0(x)\eta W - \frac{1}{2}F$	$U_0(x)\left\{\eta W - \dfrac{F}{\eta}\right\}$	$\ll U(x,y)$	$U_M(\eta W - F)$
$k(x,y)$	$U_0^2(x)K(\eta)$	$U_0^2(x)K(\eta)$	$U_d^2(x)K(\eta)$	$U_M^2 K(\eta)$
$\epsilon(x,y)$	$U_0^3(x)/xE(\eta)$	$U_0^3(x)/xE(\eta)$	$(U_d^3(x)/x)E(\eta)$	$(U_M^3/x)E(\eta)$
$\nu_t(x,y)$	$U_0(x)xD(\eta)$	$U_0(x)xD(\eta)$	$U_d(x)xD(\eta)$	$U_M xD(\eta)$
$\gamma(x,y)$	$G(\eta)$	$G(\eta)$	$G(\eta)$	$G(\eta)$
—	$U_0^2 x\int_0^\infty W^2\,d\eta = c$	$U_0^2 x\int_0^\infty \eta W^2\,d\eta = c$	$Q \equiv \left\{\int_0^\infty W\,d\eta\right\}^{-1}$	$U_M \equiv U_H - U_L$

TABLE 1. Definitions of similarity variables

	Plane jet				Round jet			
ϕ	A	B	C	S	A	B	C	S
$F(\zeta)$	0	1	0	$-DW$	0	1	0	$-\eta DW$
$W(\zeta)$	$\frac{1}{2}F$	1	0	$\eta C_{uv}K$	F	η	0	$\eta^2 C_{uv}K$
$K(\zeta)$	DW	$\frac{1}{2}F$	$\dfrac{1}{\sigma_k}$	DS_k	$2\eta DW$	F	$\dfrac{\eta}{\sigma_k}$	ηDS_k
$E(\zeta)$	$\frac{5}{2}DW$	$\frac{1}{2}F$	$\dfrac{1}{\sigma_\epsilon}$	DS_ϵ	$4\eta DW$	F	$\dfrac{\eta}{\sigma_\epsilon}$	ηDS_ϵ
$G(\zeta)$	0	$\frac{1}{2}F$	$\dfrac{1-G}{\sigma_g}$	DS_g	0	F	$\eta\dfrac{1-G}{\sigma_g}$	ηDS_g

	Plane wake				Mixing layer			
ϕ	A	B	C	S	A	B	C	S
$F(\zeta)$	—	—	—	—	0	1	0	$-DW$
$W(\zeta)$	$\dfrac{\eta}{2Q}$	1	0	0	0	$F+\eta\dfrac{U_L}{U_M}$	1	$\eta C_{uv}W'$
$K(\zeta)$	$\dfrac{D}{Q}$	$\dfrac{\eta}{2Q}$	$\dfrac{1}{\sigma_k}$	DS_k	0	$F+\eta\dfrac{U_L}{U_M}$	$\dfrac{1}{\sigma_k}$	DS_k
$E(\zeta)$	$\dfrac{2D}{Q}$	$\dfrac{\eta}{2Q}$	$\dfrac{1}{\sigma_\epsilon}$	DS_ϵ	$D\left\{W+\dfrac{U_L}{U_M}\right\}$	$F+\eta\dfrac{U_L}{U_M}$	$\dfrac{1}{\sigma_\epsilon}$	DS_ϵ
$G(\zeta)$	0	$\dfrac{\eta}{2Q}$	$\dfrac{1-G}{\sigma_g}$	DS_g	0	$F+\eta\dfrac{U_L}{U_M}$	$\dfrac{1-G}{\sigma_g}$	DS_g

The superscript, $'$, indicates differentiation with respect to ζ.

TABLE 2. Coefficients of similarity transformed equations

Source	Plane jet	Round jet
$P_{k,s}(\zeta)$	W'^2/D	W'^2/D
$P_{k,n}(\zeta)$	$C_{uv}K(0.5W+\eta W'/D)$	$C_{uv}K(W+\eta W'/D)$
$\chi(\zeta)$	0	$(K/E)^3(W'/D)^2(W-F/\eta^2)$
$\Gamma(\zeta)$	$K^{2.5}/(ED)^2W'G'$	$K^{2.5}/(ED)^2W'G'$
Source	**Plane wake**	**Mixing layer**
$P_{k,s}(\zeta)$	W'^2/D	W'^2/D
$P_{k,n}(\zeta)$	0	$\eta C_{uv}KW'/D$
$\chi(\zeta)$	0	0
$\Gamma(\zeta)$	$-K^{2.5}/(ED)^2W'G'$	$K^{2.5}/(ED)^2W'G'$

TABLE 3. Representation of source and sink terms in the ζ-coordinate

Plane jet	Round jet
$\zeta\|_0 = 0, \quad F\|_0 = 0$	$\zeta\|_0 = 0, \quad F\|_0 = 0$
$W\|_0 = 1, \quad W\|_N = W\|_{N^{-1}}\exp(Q_p)$	$W\|_0 = 1, \quad W\|_N = W\|_{N^{-1}}\exp(Q_r)$
$K'\|_0 = 0, \quad K\|_N = K\|_{N^{-1}}\exp(\sigma_k Q_p)$	$K'\|_0 = 0, \quad K\|_N = K\|_{N^{-1}}\exp(\sigma_k Q_r)$
$E'\|_0 = 0, \quad E\|_N = E\|_{N^{-1}}\exp(\sigma_\epsilon Q_p)$	$E'\|_0 = 0, \quad E\|_N = E\|_{N^{-1}}\exp(\sigma_\epsilon Q_r)$
$G'\|_0 = 0, \quad G\|_N = G\|_{N^{-1}}\exp(\sigma_g Q_p)$	$G'\|_0 = 0, \quad G\|_N = G\|_{N-1}\exp(\sigma_g Q_r)$
where $Q_p \equiv F\|_N(\zeta\|_{N^{-1}} - \zeta\|_N)/2$	where $Q_r \equiv [F/\eta]_N(\zeta\|_{N^{-1}} - \zeta\|_N)$
Plane wake	**Mixing layer**
$\zeta\|_0 = 0$	$\zeta = 0 \quad \text{at} \quad \eta = 0$
—	$F\|_0 = [\eta W]_0 + \dfrac{U_L}{U_H}[\eta W - F]_N$
$W\|_0 = 1, \quad W\|_N = W\|_{N^{-1}}\exp(Q_w)$	$W\|_0 = 1-(1-W\|_1)\exp(Q_m^-), \quad W\|_N = W\|_{N^{-1}}\exp(Q_m^+)$
$K'\|_0 = 0, \quad K\|_N = K\|_{N^{-1}}\exp(\sigma_k Q_w)$	$K\|_0 = K\|_1\exp(\sigma_k Q_m^-), \quad K\|_N = K\|_{N^{-1}}\exp(\sigma_k Q_m^+)$
$E'\|_0 = 0, \quad E\|_N = E\|_{N^{-1}}\exp(\sigma_\epsilon Q_w)$	$E\|_0 = E\|_1\exp(\sigma_\epsilon Q_m^-), \quad E\|_N = E\|_{N^{-1}}\exp(\sigma_\epsilon Q_m^+)$
$G'\|_0 = 0, \quad G\|_N = G\|_{N^{-1}}\exp(\sigma_g Q_w)$	$G\|_0 = G\|_1\exp(\sigma_g Q^{-m}), \quad G\|_N = G\|_{N^{-1}}\exp(\sigma_g Q_m^+)$
where	where $Q_m^- \equiv \left[F + \dfrac{U_L\eta}{U_H - U_L}\right]_0(\zeta\|_1 - \zeta\|_0),$
$Q_w \equiv \eta\|_N(\zeta\|_{N^{-1}} - \zeta\|_N)/(2Q)$	$Q_m^+ \equiv \left[F + \dfrac{U_L\eta}{U_H - U_L}\right]_N(\zeta\|_{N^{-1}} - \zeta\|_N)$

TABLE 4. Summary of boundary conditions in the ζ-coordinate

C_μ	$C_{\mu g}$	m	C_{uv}	σ_k	σ_ϵ	σ_g
0.09	0.10	3.0	0.33	1.00	1.00	1.00
$C_{\epsilon 1}$	$C_{\epsilon 2}$	$C_{\epsilon 3}$	$C_{\epsilon 4}$	C_{g1}	C_{g2}	C_{g3}
1.44	1.92	0.30	0.10	1.60	0.15	0.16

TABLE 5. Values of model constants

was determined using the experimental data of plane jets (Bradbury 1965; Gutmark & Wygnanski 1976) near the region where $\gamma \approx 0.5$, and it turns out to be about 0.10. A number of trial computations revealed that the spreading rate and the Reynolds shear stress are more sensitive to $C_{\epsilon 4}$ than to C_{g3}, which permitted relatively easy determination of the constant $C_{\epsilon 4} = 0.1$ to reproduce the measured spreading rate of

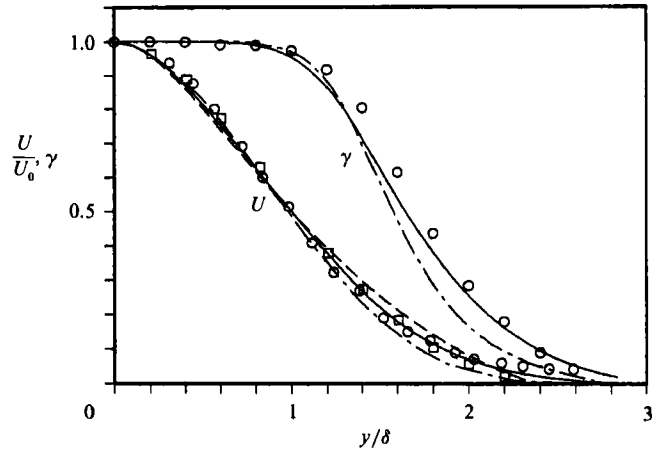

FIGURE 2. The streamwise mean velocity and the intermittency factor profiles for the plane jet. ——, present $k-\epsilon-\gamma$ model; ——, $k-\epsilon$ model of Hanjalic & Launder (1980); ———, CRSM of Byggstoyl & Kollmann (1986): ○, data of Gutmark & Wygnanski (1976); □, data of Heskestad (1965).

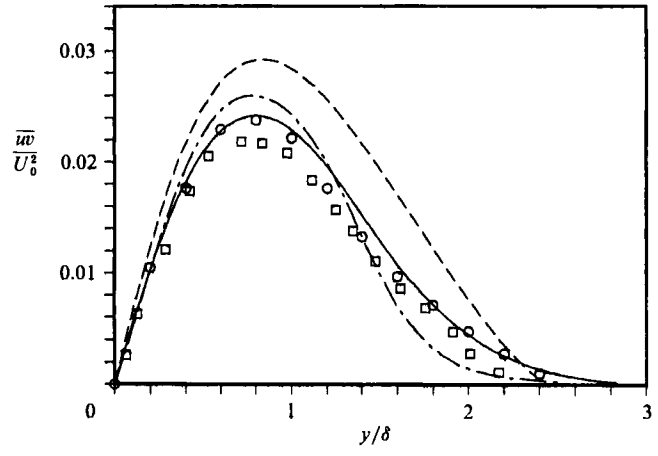

FIGURE 3. The Reynolds shear stress profiles for the plane jet. Notations as in figure 2.

the plane jet in Gutmark & Wygnanski (1976), and then C_{g3} was selected to be 0.16 by referring to the experimental intermittency factor profile. Note that these three values were selected based only on plane jet experiments. A preliminary calculation of the round jet with $C_{\epsilon 3} = 0$ yielded a spreading rate of 0.094 which is lower than 0.098 by the HL model, but it is still higher than the experimental value of 0.086. The correct prediction is obtained when the constant of Pope's vortex stretching model $C_{\epsilon 3}$ is about 0.3, much lower than the originally suggested value of 0.79.

Figures 2, 3 and 4 show profiles of mean velocity and turbulence quantities in the plane jet. The computational results by employing the present $k-\epsilon-\gamma$ model, HL's $k-\epsilon$ model, and Byggstoyl & Kollmann's (1986) conditional Reynolds stress model (hereinafter referred to as CRSM) are presented together with the experimental data. The mean velocity profiles in figure 2 are compared with the HWA (hot-wire anemometer) data of Heskestad (1965) and Gutmark & Wygnanski (1976). The prediction with the HL model is slightly higher than experiments in the outer region, whereas the CRSM gives lower values. The present result lies in between these two

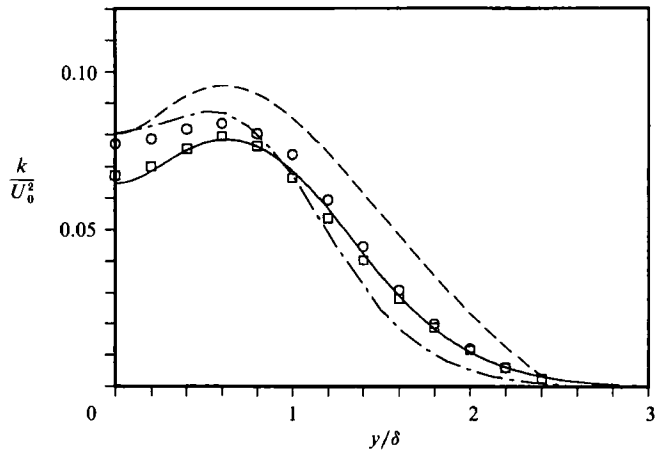

FIGURE 4. The turbulent kinetic energy profiles for the plane jet. Notations as in figure 2.

profiles, and is in good agreement with the experiments. A comparison of the intermittency factor in figure 2 shows that the present mass entrainment model performs better than the original version of Byggstoyl & Kollmann (1986). For the Reynolds shear stress in figure 3, our $k-\epsilon-\gamma$ model yields a profile closest to the experimental data among the three models. The same is true for the turbulent kinetic energy profile as shown in figure 4. The profiles of k and $\overline{uv}$ with the CRSM drop too rapidly in the outer intermittent region. Because of the less reliable HWA data in this region owing to the existence of backflows and large velocity fluctuations, Looney & Walsh (1984) argued that the assessment of turbulence models must be based on a comparison with data within $y < 1.6\delta$. However, recent LDA (laser-Doppler anemometer) data of Ramaprian & Chandrasekhara (1985) for a water jet are nearly the same as previous HWA data in this region for Reynolds shear stress and the estimated turbulent kinetic energy by $k = 0.75\,(\overline{u^2}+\overline{v^2})$. For the spreading rate, Rodi (1975) suggests a value of 0.11, but Looney & Walsh (1984) and Haworth & Pope (1987) recommend a value of 0.10 after surveying a number of recent experiments. The present model correctly produces this latter one, but HL's model and the CRSM give 0.116 and 0.108, respectively. However, since the new constant $C_{\epsilon 4}$ has been adjusted against the spreading rate, the present prediction only proves that the constant $C_{\epsilon 4}$ has been properly assigned. The index for decay rate of the centreline mean velocity is defined as $K_{\mathrm{up}} \equiv \partial(J_\infty/U_c^2)/\partial x$, where J_∞ is the momentum flux in the self-preserving region. The value of K_{up} summarized by Ramaprian & Chandrasekhara is in the range of 0.16–0.17 when the extreme values are discarded. The present $k-\epsilon-\gamma$ model gives a value of 0.169, but HL's model yields 0.206, which is much higher than the experimental upper bound.

Computations of the round jet in stagnant surroundings are presented in figures 5, 6 and 7. The computational results by employing the present $k-\epsilon-\gamma$ model, HL's $k-\epsilon$ model, Janicka & Kollmann's (1983) CRSM and Pope's (1978) $k-\epsilon$ model are compared with the HWA data of Wygnanski & Fiedler (1969) and Rodi (1975). The mean velocity profiles are shown in figure 5. The prediction with the CRSM is lower than experiments in the outer region. HL's and Pope's models follow the data of Wygnanski & Fiedler, whereas the present model follows the data of Rodi which were recommended as more reliable ones (Rodi 1975). As in the plane jet, the present mass entrainment model significantly improves the predictability for the intermittency factor of the round jet (figure 5). The differences in the predicted maximum Reynolds

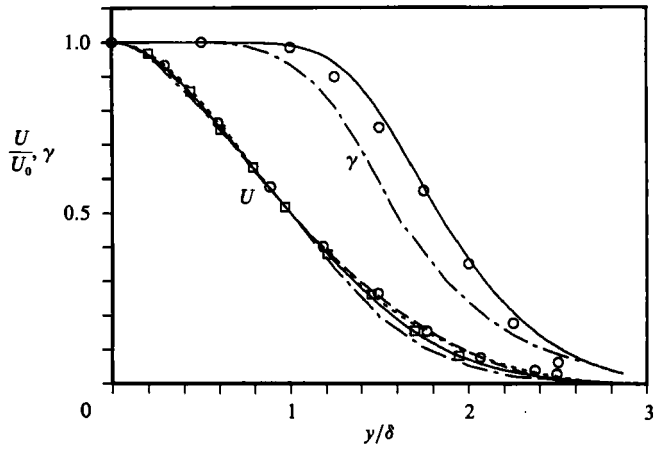

FIGURE 5. The streamwise mean velocity and the intermittency factor profiles for the round jet. ——, present $k-\epsilon-\gamma$ model; — —, $k-\epsilon$ model of Hanjalic & Launder (1980); – – –, $k-\epsilon$ model of Pope (1978); — — —, CRSM of Janicka & Kollmann (1983): ○, data of Wygnanski & Fiedler (1969); □, data of Rodi (1975).

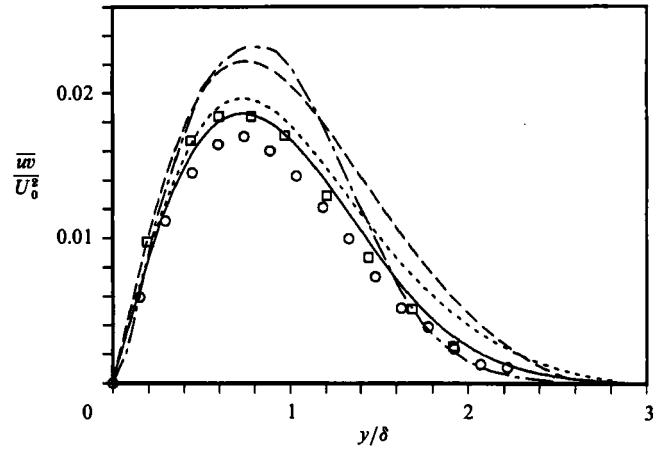

FIGURE 6. The Reynolds shear stress profiles for the round jet. Notations as in figure 5.

shear stress as in figure 6 are quite remarkable; only the present model gives the correct peak value. The profiles for the turbulent kinetic energy are compared in figure 7. The present $k-\epsilon-\gamma$ model and Pope's model provide similar distributions of k in the whole region, which are good only in the outer region. The present centreline value of 0.072 is much lower than the hot-wire data, but is very close to the recent LDA data by Komori & Ueda (1985) as shown in figure 7. Note that, although their measurements were made in a coflowing jet, the centreline value must be comparable to that in the round jet in stagnant surroundings, because the mean velocity and the Reynolds shear stress are approximately the same as those of Rodi (1975) at the same streamwise locations. For the spreading rate, only the present and Pope's models give the correct value of about 0.086, but the HL model yields 0.098 and CRSM predicts a higher value of about 0.11. Here, it should be noted that Pope's model constant was adjusted with respect to the spreading rate of this round jet. The decay rate for the centreline mean velocity defined as $K_{ur} \equiv \partial(U_{exit}/U_c)/\partial(x/D)$, is calculated to be 0.179 with the present model, which falls in the experimental range

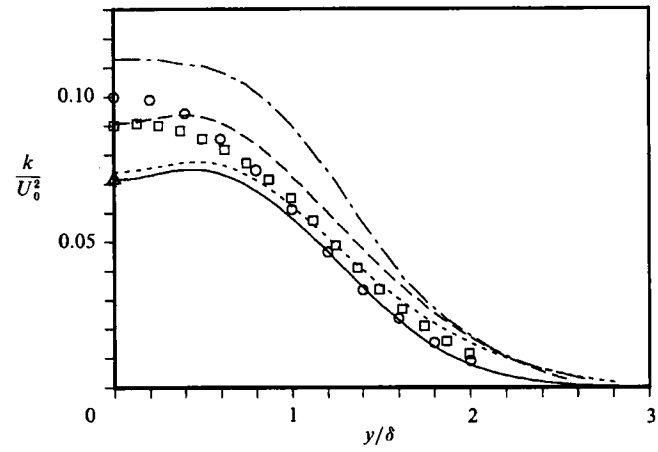

FIGURE 7. The turbulent kinetic energy profiles for the round jet. △, data of Komori & Ueda (1985). Other notations as in figure 5.

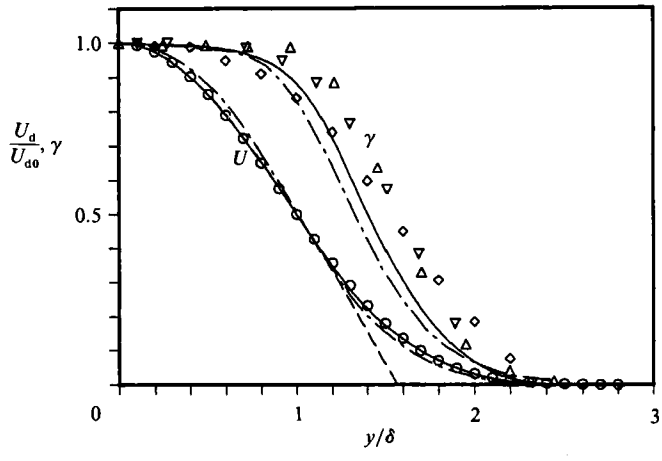

FIGURE 8. The streamwise mean defect velocity and the intermittency factor profiles for the plane wake. ——, present $k-\epsilon-\gamma$ model; — —, $k-\epsilon$ model of Hanjalic & Launder (1980); – – –, CRSM of Byggstoyl & Kollmann (1986): ○, □, symmetrical airfoil & solid strip data Wygnanski *et al.* (1986), respectively; ◇, data of Thomas (1973); ▽, data of LaRue (1974); △, data of Fabris (1979).

of 0.169–0.185 by Wygnanski & Fiedler (1969). Both HL's model and the CRSM yield about 0.22 which is significantly higher than the upper bound of the experimental range.

Computations for a plane far wake with the three models are compared with the recent HWA data of Wygnanski, Champagne & Marasli (1986, hereinafter referred to as WCM). They investigated the effect of the wake generator on the downstream developments of the mean and turbulence quantities. Their major finding is that the normalized mean velocity is independent of the wake generator, but the turbulence intensity depends on it. The mean defect velocity profiles are compared with the data of a symmetrical airfoil in figure 8. The agreement is good for the $k-\epsilon-\gamma$ model; the CRSM shows slightly distorted shape; and the profile with HL model drops too rapidly in the outer intermittent region. The calculated intermittency factor profiles are compared with the data of Thomas (1973), LaRue (1974) and Fabris (1979) in

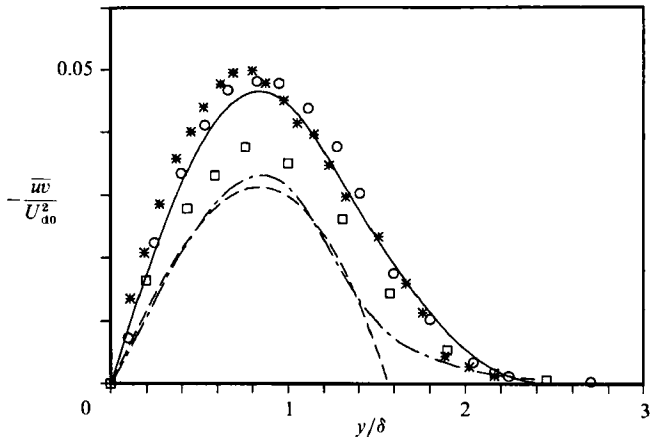

FIGURE 9. The Reynolds shear stress profiles for the plane wake. ✱, data of Pot (1979). Other notations as in figure 8.

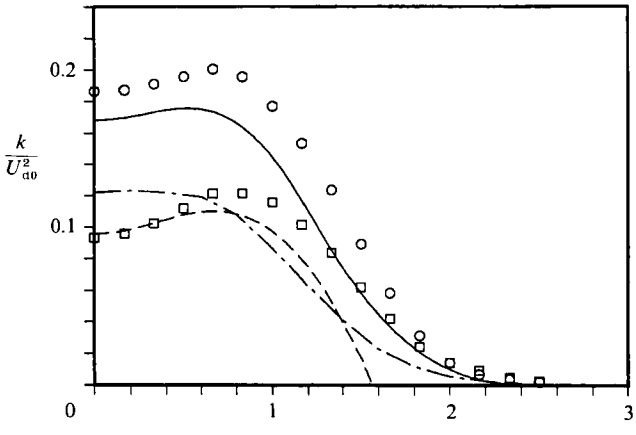

FIGURE 10. The turbulent kinetic energy profiles for the plane wake. Notations as in figure 8.

figure 8. It can be seen that the present model allows more accurate prediction than the CRSM. Figure 9 represents the predicted and the measured Reynolds shear stress profiles. Two data sets obtained for the symmetrical airfoil and the solid strip by WCM are presented for comparison. The far-wake data behind a symmetrical airfoil by Pot (1979) which has been recommended as a target profile in the 1980–81 Stanford conference by Patel (SCP80, pp. 340–345) are also included. Clearly, the present model compares most favourably with the experiments, but the CRSM and HL models give significantly lower values, which imply that both models predict too small momentum transport. The improvement achieved by the present prediction is mainly due to the presence of the interaction model in the dissipation equation which decreases the level of dissipation, thereby increasing the momentum transport. Note that the interaction model results in a decrease of momentum transport in the jet flows in comparison with other models as shown in figures 3 and 6. Figure 10 depicts the turbulent kinetic energy profiles. It is pointed out by Rodi (1975) and Thomas (1973) that past measurements of k in the far wake are hardly reliable. WCM reports only the distributions of $\overline{u^2}$ for both the symmetrical airfoil and the solid strip. Hence, we have estimated the turbulent kinetic energy by using the

approximations of Townsend (1975, p. 107) that $\overline{u^2}/\overline{w^2} = 1.3$ and $\overline{u^2}/\overline{v^2} = 1.6$. Such approximate estimations are represented in figure 10 for rough comparison with the predictions. The prediction with the $k-\epsilon-\gamma$ model lies in between the two data sets; but the predictions with the HL model and CRSM are notably lower than the experiments in the outer region. The calculated spreading rate, $S_w \equiv \partial(0.5U_\infty \delta/U_d)/\partial x$ defined by Rodi (1975), turned out to be 0.0925 with the $k-\epsilon-\gamma$ model. This value is a little lower than 0.098 which was recommended at the Stanford conference, but it is within the range 0.08–0.10 measured by WCM. The spreading rate with the HL model is only about 0.06. Since the Reynolds shear stress level by CRSM is nearly the same as that of the HL model, the spreading rate with CRSM is also significantly underpredicted. The decay rate of the centreline defect-velocity, $K_{uw} \equiv U_d/U_\infty(x/\theta)$ defined by WCM, varies in a range 1.56–1.88 in experiments for different wake generators. Here, θ stands for the momentum thickness. The predicted values are 1.626 with the $k-\epsilon-\gamma$ model and 2.089 with HL model. These two parameters confirm the superiority of the $k-\epsilon-\gamma$ model over the HL model and CRSM.

Plane mixing layers with values of the velocity ratio, R, between 0 and 0.9 have been investigated. Here, R is the ratio of the lower free-stream speed U_L to the higher one U_H. As noted by Rodi (1975) and Haworth & Pope (1987), a plane mixing layer requires a long streamwise distance to attain full development of turbulence quantities. And the spreading rate and the turbulent structures are highly sensitive to the initial and the boundary conditions. Hence, the disagreement among the experiments is notable especially in the case of $R = 0$. Keeping this fact in mind, a comparison is made between the computational results and some typical experiments. In the 1980–81 Stanford Conference, Birch (SCP80, p. 170) recommended a spreading rate relation of $dL/dx = 0.115\ (1-R)/(1+R)$ after surveying experimental data. L is the distance between the points where $U = 0.9^{\frac{1}{2}}\ (U_H-U_L)+U_L$ and $U = 0.1^{\frac{1}{2}}\ (U_H-U_L)+U_L$. The variation of the calculated spreading rates with the change of the velocity ratio is compared in figure 11 (*a*) with Birch's correlation. The predicted variation of the spreading rate by the $k-\epsilon-\gamma$ model almost coincides with Birch's experimental correlation, where the HL model underpredicts the spreading rates for all values of $R < 1.0$. In the case of $R = 0$, $dL/dx = 0.118$ with the $k-\epsilon-\gamma$ model and it is 0.100 with the HL model. When the shear-layer thickness is defined as $\delta = |y_{0.1}-y_{0.9}|$, Rodi (1975) recommends that $d\delta/dx = 0.16$. It is calculated as 0.163 with the $k-\epsilon-\gamma$ model and as 0.160 with HL model. The predicted peak values of the Reynolds shear stress are plotted in figure 11 (*b*). For the case of $R = 0$, the peak values are 0.0125 with the $k-\epsilon-\gamma$ model, and 0.011 with the HL model. Both these values are within the range of experimental data, 0.008 (Hussain & Husain 1980) and 0.0137 (Sunyach & Mathieu 1969). Such wide scattering of the measured values does not allow us to make any conclusive judgement about the performance of each model. A theoretical analysis for the relationship between the Reynolds shear stress and the mean velocity profile has been done by Townsend (1976, pp. 227–230) and Pui & Gartshore (1979). Their relationship is

$$\overline{uv}_{max}/(U_H-U_L)^2 = 0.078\ (d\delta/dx)\ (1+R)/(1-R).$$

For internal consistency, the normalized maximum shear stress must be 0.0125 for the experimentally measured spreading rate of 0.160. This value is the same as the one predicted by the present model.

The computational results for a plane mixing layer with a velocity ratio of $R = 0.5$ are compared with the recent data of Mehta & Westphal (1986). The mean velocity

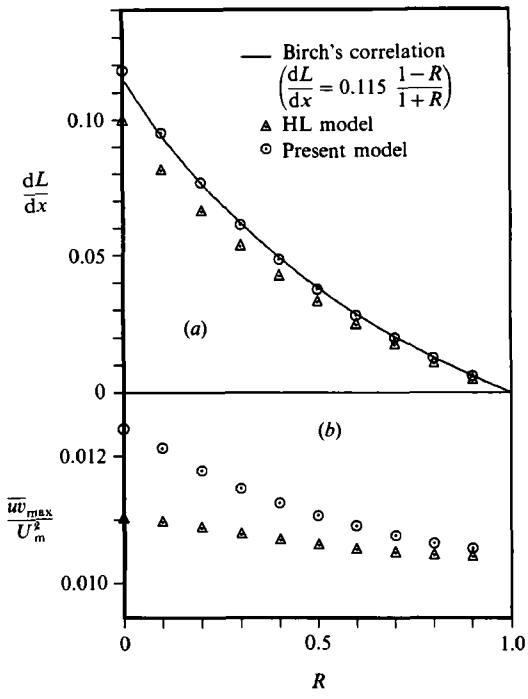

FIGURE 11. The changes of the spreading rate, (*a*) and the maximum Reynolds shear stress, (*b*) for the plane mixing layer with a velocity ratio R.

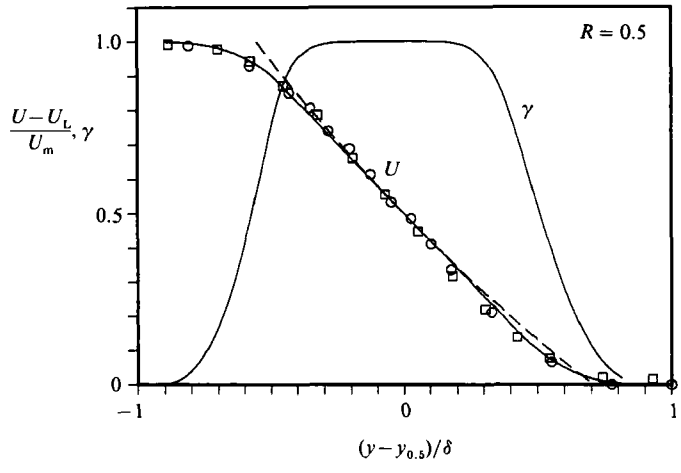

FIGURE 12. The streamwise mean velocity and the intermittency factor profiles for the mixing layer with $R = 0.5$. ——, present $k-\varepsilon-\gamma$ model; — —, $k-\varepsilon$ model of Hanjalic & Launder (1980): ○, □, two data set of Mehta & Westphal (1986).

profile in figure 12 calculated with the HL model shows too fast approach to the free-stream velocity at the high-velocity edge, and slower variation in the low-velocity side. The result with the present model matches satisfactorily with experimental data over the whole layer. The calculated intermittency factor profile is also included in figure 12. The Reynolds shear stress and turbulent kinetic energy profiles are compared in figures 13 and 14 respectively. Since Mehta & Westphal do

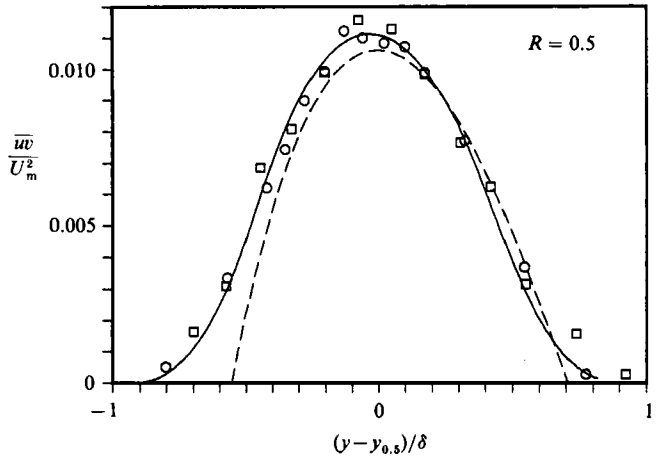

FIGURE 13. The Reynolds shear stress profiles for the mixing layer with $R = 0.5$. Notations as in figure 12.

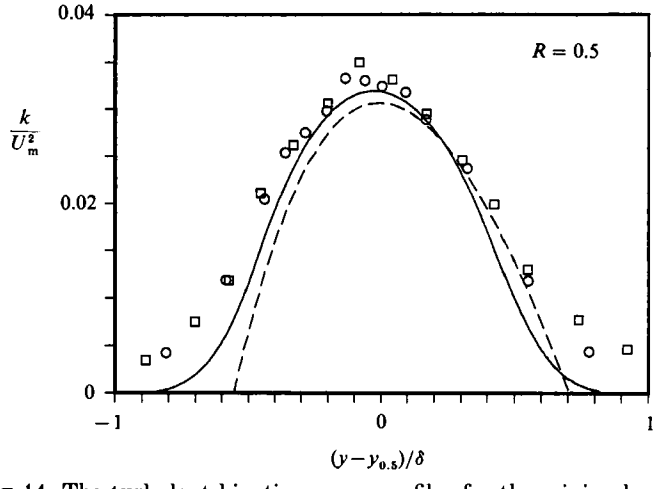

FIGURE 14. The turbulent kinetic energy profiles for the mixing layer with $R = 0.5$. Notations as in figure 12.

not report $\overline{w^2}$ distribution, the turbulent kinetic energy is estimated by $k = 0.75(\overline{u^2}+\overline{v^2})$. The present model predicts much improved profiles for both $\overline{uv}$ and k in the high-velocity side. The new eddy-viscosity relation increases the momentum transport in the intermittent edge region, thereby the profile shape changes smoothly in that region. In a viewpoint of the interaction model, the high- and low-velocity sides are similar to wake and jet flows, respectively. The interaction model dictates the decrease of dissipation in the high-velocity side, so the turbulence intensity increases there. The converse is true in the low-velocity side.

6. Concluding remarks

A physical model for the interaction between the mean shear and intermittency fields has been proposed in order to remedy the various anomalies in predicting turbulent jets, wakes and mixing layers. The proposed model is incorporated in the

dissipation rate and intermittency equations. Also a new eddy-viscosity model accounting for bulk convective transport by the mean velocity jump between the turbulent and irrotational fluids is formulated. The modelled equations are applied to the turbulent free shear flows mentioned above. The computed profiles for the mean velocity, the intermittency factor, the Reynolds shear stress, and the turbulent kinetic energy are favourably compared with available experiments. The proposed eddy viscosity relation permits more momentum transport in the intermittent region, especially for the wake and the mixing layer, than previous models, thereby the mean velocity and the Reynolds shear stress profiles are satisfactorily predicted. The interaction model increases the dissipation rate for the jets, and decreases it for the wake. The peak values of the Reynolds shear stresses are predicted very closely to the experimental values for all turbulent free shear flows considered. Hence, the anomalies in predicting the spreading rates are satisfactorily resolved. Comparisons of the intermittency factor indicate that the addition of the interaction term in the mass entrainment model improves the predictability.

In contrast to the method of the Kollmann group (1981, 1983, 1986) based on the zone-averaged stress equations, the present work is based on the conventional Reynolds averaged equations. The overall agreement of the computational results with the experimental data supports the present approach of taking into account the intermittent nature of the flow. Although this approach loses much information on the dynamics of turbulent and irrotational fluids, it is more economical in the sense that it halves the number of partial differential equations to be solved.

The similarity solution method of Paullay *et al.* (1985) has been adopted in obtaining all numerical solutions reported in this paper. Although this method was originally applied to plane and radial jets by them, it also works very well for the round jet, the plane wake and the plane mixing layer. Solutions with usual numerical marching techniques, such as the finite-difference procedure of Patankar & Spalding (1970), inevitably involve numerical errors (Launder & Morse 1979). Therefore, the similarity solution method is preferable in comparing the performance of turbulence models for self-preserving flows.

In this paper, the proposed $k-\epsilon-\gamma$ equation model has been applied only for free shear flows. Recently, preliminary tests of the model have been done against various wall bounded flows, and it has been found that the present model is also capable of describing the flow field between a wall boundary and a free or a symmetric boundary. Further study is required to pursue its applicability for a wider range of wall-bounded shear flows.

The authors wish to thank the reviewers for their invaluable comments and suggestions which led to improvements in the quality of this paper.

REFERENCES

Bradbury, L. J. S. 1965 The structure of a self-preserving turbulent plane jet. *J. Fluid Mech.* **23**, 31.

Byggstoyl, S. & Kollmann, W. 1981 Closure model for intermittent turbulent flows. *Intl J. Heat Mass Transfer* **24**, 1811.

Byggstoyl, S. & Kollmann, W. 1986 A closure model for conditioned stress equations and its application to turbulent shear flows. *Phys. Fluids* **29**, 1430.

Chevray, R. & Tutu, N. K. 1978 Intermittency and preferential transport of heat in a round jet. *J. Fluid Mech.* **88**, 133.

Dopazo, C. 1977 On conditioned averages for intermittent turbulent flows. *J. Fluid Mech.* **81**, 433.

FABRIS, G. 1979 Conditional sampling study of the turbulent wake of a cylinder. Part 1. *J. Fluid Mech.* **94**, 673.

GUTMARK, E. & WYGNANSKI, I. 1976 The planar turbulent jet. *J. Fluid Mech.* **73**, 465.

HANJALIC, K. & LAUNDER, B. E. 1980 Sensitizing the dissipation equation to irrotational strains. *Trans. ASME* I: *J. Fluids Engng* **102**, 34.

HANJALIC, K., LAUNDER, B. E. & SCHIESTEL, R. 1980 Multiple-time-scale concepts in turbulent transport modelling. In *Turbulent Shear Flows 2* (ed. L. J. S. Bradbury, F. Durst, B. E. Launder, F. W. Schmidt & J. H. Whitelaw), pp. 36–49, Springer.

HAWORTH, D. C. & POPE, S. B. 1987 A pdf modeling study of self-similar turbulent free shear flows. *Phys. Fluids* **30**, 1026.

HESKESTAD, G. 1965 Hot-wire measurements in a plane turbulent jet. *J. Appl. Mech.* **32**, 1.

HUANG, G. P. G. 1986 The consumption of elliptic turbulent flows with second-moment closure models. PhD thesis, University of Manchester.

HUSSAIN, A. K. M. F. & HUSAIN, Z. D. 1980 Turbulence structure in the axisymmetric free mixing layer. *AIAA J.* **18**, 1462.

JANICKA, J. & KOLLMANN, W. 1983 Reynolds-stress closure model for conditional variables. In *Turbulent Shear Flows 4* (ed. L. J. S. Bradbury, F. Durst, B. E. Launder, F. W. Schmidt & J. H. Whitelay), pp. 73–86. Springer.

KLINE, S. J., CANTWELL, B. & LILLEY, G. K. (eds) 1981/82 Comparison of computation and experiment. *Proc. 1980–81 AFOSR–HTTM–Stanford Conference on Complex Turbulent Flows.* Stanford.

KOLLMANN, W. & JANICKA, J. 1982 The probability density function of a passive scalar in turbulent shear flows. *Phys. Fluids* **25**, 1755.

KOMORI, S. & UEDA, H. 1985 The large-scale coherent structure in the intermittent region of the self-preserving round free jet. *J. Fluid Mech.* **152**, 337.

LARUE, J. C. 1974 Detection of the turbulent–nonturbulent interface in slightly heated turbulent shear flows. *Phys. Fluids* **17**, 1513.

LAUNDER, B. E. 1984 Progress and prospects in phenomenological turbulence models. In *Theoretical Approaches to Turbulence* (ed. D. L. Dwoyer *et al.*) pp. 155–186. Springer.

LAUNDER, B. E. & MORSE, A. P. 1979 Numerical prediction of axisymmetric free shear flows with a Reynolds stress closure. In *Turbulent Shear Flows 1* (ed. F. Durst, B. E. Launder, F. W. Schmidt & J. H. Whitelaw), pp. 279–294. Springer.

LAUNDER, B. E., MORSE, A. P., RODI, W. & SPALDING, D. B. 1972 Prediction of free shear flows – a comparison of six turbulence models. *NASA SP 321.*

LAUNDER, B. E., REECE, G. J. & RODI, W. 1975 Progress in the development of a Reynolds-stress turbulence closure. *J. Fluid Mech.* **68**, 537.

LIBBY, P. A. 1975 On the prediction of intermittent turbulent flows. *J. Fluid Mech.* **68**, 273.

LIBBY, P. A. 1976 Prediction of the intermittent turbulent wake of a heated cylinder. *Phys. Fluids* **19**, 494.

LOONEY, M. K. & WALSH, J. J. 1984 Mean-flow and turbulent characteristics of free and impinging jet flows. *J. Fluid Mech.* **147**, 397.

LUMLEY, J. L. 1980 Second order modelling of turbulent flows. In *Prediction Methods for Turbulent Flows* (ed. W. Kollmann), pp. 1–31. Hemisphere.

MCGUIRK, J. J. & RODI, W. 1977 The calculation of three-dimensional turbulent free jets. In *Turbulent Shear Flows 1* (ed. F. Durst, B. E. Launder, F. W. Schmidt & J. H. Whitelaw), pp. 71–83. Springer.

MEHTA, R. D. & WESTPHAL, R. V. 1986 Near-field turbulence properties of single- and two-stream plane mixing layers. *Exps Fluids* **4**, 257.

MORSE, A. P. 1977 Axisymmetric turbulent shear flows with and without swirl. PhD thesis, University of London.

PATANKAR, S. V. & SPALDING, D. B. 1970 *Heat and Mass Transfer in Boundary Layers*, 2nd edn. London: Intertext.

PATEL, V. C. & SCHEUERER, G. 1982 Calculation of two-dimensional near and far wakes. *AIAA J.* **20**, 900.

PAULLAY, A. J., MELNIK, R. E., RUBEL, A., RUDMAN, S. & SICLARI, M. J. 1985 Similarity solutions for plane and radial jets using a $k-\epsilon$ turbulence model. *Trans. ASME* I: *J. Fluids Engng* **107**, 79.

POPE, S. B. 1978 An explanation of the turbulent round-jet/plane-jet anomaly. *AIAA J.* **16**, 279.

POPE, S. B. 1984 Calculation of a plane turbulent jet. *AIAA J.* **22**, 896.

POT, P. J. 1979 Measurements in a 2D wake merging into a boundary layer. *National Luchten Ruimtevaartlaboratorium* TR 19063 U.

PUI, N. K. & GARTSHORE, I. S. 1979 Measurements of growth rate and structure in plane turbulent mixing layers. *J. Fluid Mech.* **91**, 111.

RAJARATNAM, N. 1976 *Turbulent Jets.* Elsevier.

RAMAPRIAN, B. R. & CHANDRASEKHARA, M. S. 1985 LDA measurements in plane turbulent jets. *Trans. ASME* I: *J. Fluids Engng* **107**, 264.

RODI, W. 1972 The prediction of free turbulent boundary layers by use of a two-equation model of turbulence. PhD thesis, University of London.

RODI, W. 1975 A review of experimental data of uniform density free turbulent boundary layers. In *Studies in Convection* (ed. B. E. Launder), vol. 1, pp. 79–165. Academic.

SOHN, C. H., CHOI, D. H. & CHUNG, M. K. 1991 Calculation of plane of symmetry flow with a modified form of the $k-\epsilon$ model. *AIAA J.* **29**, 591.

STUTTGEN, W. & PETERS, N. 1987 Stability of similarity solutions by two-equation models of turbulence. *AIAA J.* **25**, 824.

SUNYACH, M. & MATHIEU, J. 1969 Zone de melange d'un jet plan; fluctuations induites dans le cone a potentiel – intermittence. *Intl J. Heat Mass Transfer* **12**, 1679.

TENNEKES, H. & LUMLEY, J. L. 1972 *A First Course in Turbulence.* MIT Press.

THOMAS, R. M. 1973 Conditional sampling and other measurements in a plane turbulent wake. *J. Fluid Mech.* **57**, 549.

TOWNSEND, A. A. 1976 *The Structure of Turbulent Shear Flow.* Cambridge University Press.

WYGNANSKI, I. & FIEDLER, H. E. 1969 Some measurements in the self-preserving jet. *J. Fluid Mech.* **38**, 577.

WYGNANSKI, I., CHAMPAGNE, F. & MARASALI, B. 1986 On the large-scale structures in two-dimensional, small-deficit, turbulent wakes. *J. Fluid Mech.* **168**, 31.